Infrared Physics & Technology 52 (2009) 235–240

Contents lists available at ScienceDirect

Infrared Physics & Technology

journal homepage: www.elsevier.com/locate/infrared

Mid-wave QWIPs for the [3–4.2 μm] atmospheric window

Vincent Guériaux *, Alexandru Nedelcu, Mathieu Carras, Odile Huet, Xavier Marcadet, Philippe Bois

Alcatel-Thales III–V Lab, Campus de Polytechnique, 1 Avenue Augustin Fresnel, 91767 Palaiseau Cedex, France

ARTICLE INFO

Article history:
Available online 12 June 2009

Keywords:
QWIP
Mid-infrared
InP
GaAs
Detector

ABSTRACT

We report two approaches using Quantum Well Infrared Photodetectors for detection in the [3–4.2 μm] atmospheric window. Taking advantage of the large band gap discontinuity we demonstrated a strained AlInAs/InGaAs heterostructure on InP. The optical coupling in this structure has been experimentally and numerically investigated. The results show that the coupling is mainly due to guided modes. The second approach is based on double barrier strained AlGaAs/AlAs/GaAs/InGaAs active layers on GaAs. The segregation of the elements III in these structures has been investigated using a transmission electron microscope. The results show a strong modification of the conduction band profile. We demonstrate peak wavelengths at 3.9 μm for the InP based detector and 4.0 μm for the GaAs based detector. We report a background limited peak detectivity (2π field of view, 300 K background) at 4.0 μm of about 2×10^{11} cm $Hz^{1/2}$ W^{-1} at 77 K, and 1.5×10^{11} cm $Hz^{1/2}$ W^{-1} at 100 K.

1. Introduction

Quantum Well Infrared Photodetectors (QWIPs) have been widely investigated for detection in the long-wave (LW) infrared [8–14 μm] region of the infrared spectrum [1]. Their specific advantages (GaAs-based III–V materials, easy wavelength adjustment, high thermal stability, high uniformity and yield, no low-frequency noise) established them as high performance detectors for third generation infrared cameras. A widely claimed advantage for QWIPs is the so-called band-gap engineering and versatility of the III–V processing allowing the custom design of quantum structures to detect into a large spectral range. Although LW QWIPs became an industrial solution for thermal imagers, there has been a smaller amount of work in mid-wave (MW) QWIPs.

MW QWIPs have been studied for the most part in the [4.3–5 μm] atmospheric window. This is due to the spectral radiance of near 300 K objects, and to energy transitions easier to obtain. Schneider et al. [2] developed a 4.4 μm peak responsivity detector using strained $Al_{0.32}Ga_{0.68}As/In_{0.3}Ga_{0.7}As$ quantum wells (QW) on GaAs. To broaden the responsivity spectrum, Gunapala et al. [3] proposed the use of coupled $Al_{0.3}Ga_{0.7}As/GaAs/In_{0.3}Ga_{0.7}As$ quantum wells structures with peak detection at 4.6 μm. Using double barrier strained (DBS) $Al_{0.37}Ga_{0.63}As/AlAs/GaAs/In_{0.16}Ga_{0.84}As$ QWIPs, Fiore et al. [4] demonstrated a peak responsivity at 4.5 μm. QWIPs have also been demonstrated at 4.9 μm with the InGaAs/InGaP heterostructure on InP [5], and at 5.5 μm with InGaAs/AlGaAsP on GaAs [6].

Detection in the [3–4.2 μm] window is also very interesting, due to the better atmospheric transmission in comparison with the [4.3–5 μm] and the [8–14 μm] windows. Moreover, lower wavelengths lead to a lower diffraction limit, thus the optics can be reduced (size and weight) at constant magnification. And for detection below 3.5 μm materials such as fused silica, quartz and BK7 can be used for the lens manufacturing. Also, as the working temperature increase with the wavelength reduction, the constraints on the cooling machine are reduced. In addition, detection in this spectral range is interesting for various applications such as gas detection at 3.2 μm for CH_4 and 4.25 μm for CO_2.

Various systems of alloys/substrates have been used for detection in the [3–4.2 μm] atmospheric window. Intersubband transitions were reported at 4.2 μm in GaN/AlGaN QW on sapphire [7] and at 3.25 μm with ZnO/MgZnO on ZnO [8]. Using the MgSe/ZnCdSe alloy on InP, Li et al. [9] measured intersubband absorptions in the spectral range [3.3–4.9 μm]. Another approach was proposed by E. Luna et al. with the AlGaAs/AlAs/GaAsN heterostructure on GaAs [10]. Beyond these absorption demonstrations, there have been much fewer photo-response studies on QWIPs in this spectral range. Thanks to the large band gap discontinuity of the $In_{0.53}Ga_{0.47}As/Al_{0.52}Ga_{0.48}As$ heterostructure on InP, Ozer et al. [11] demonstrated the first large format focal plane array (FPA) at 4.2 μm.

In this paper we report two different approaches using Quantum Well Infrared Photodetectors for detection in the [3–4.2 μm] atmospheric window. Taking advantage of the large band gap discontinuity we demonstrated a strained AlInAs/InGaAs heterostructure on InP. We experimentally and numerically investigate the optical coupling in such structures. The second approach is based on double barrier strained AlGaAs/AlAs/GaAs/InGaAs active layers

* Corresponding author.
E-mail address: vincent.gueriaux@3-5lab.fr (V. Guériaux).

1350-4495/$ - see front matter © 2009 Elsevier B.V. All rights reserved.
doi:10.1016/j.infrared.2009.05.037

on GaAs [12]. We report a strong influence of the segregation process on the composition profile and on the electrical characteristics.

2. Strained QWIP on InP

The sample was grown on a semi-insulating InP substrate, using molecular beam epitaxy (RIBER 49 system). The active layer consists of 10 periods of the following sequence: $Al_{0.48}In_{0.52}As$ (20 nm)/$In_{0.59}Ga_{0.41}As$ (3.5 nm). The wells are slightly strained on InP and nominally doped with silicon to 1.10^{12} cm^{-2}. The active layer is sandwiched between doped $In_{0.53}Ga_{0.47}As$ contact layers. 100×100 μm^2 and 50×50 μm^2 mesa pixels were defined using dry-etching techniques. Two-dimensional gratings with various periods were etched in the upper contact layer. Pixels without optical coupling structure are also available, on the same test cell. Standard ohmic contacts were defined on top of the pixels and on the common bottom $In_{0.53}Ga_{0.47}As$ contact. The sample was mounted in a liquid helium cooled laboratory cryostat with an f-number equal to 1.6 and an uncoated ZnSe window. The responsivity spectra were measured with a Fourier Transform IR interferometer (FTIR) (Nicolet Avatar 360). The sample was used as an external detector and illuminated with a collimated beam through the InP substrate.

Fig. 1 shows spectral responsivities of the sample at various angles of incidence. The responsivities were recorded for angles from $-18°$ to 18° between the FTIR collimated beam and the normal at the InP substrate. At normal incidence we report a peak wavelength at 3.9 μm and a full width at half maximum of 0.3 μm. This responsivity is fully comprised in the [3–4.2 μm] atmospheric window.

As presented in Fig. 1 the recorded spectra are symmetric with respect to the incident angle. The high frequency oscillations superimposed on the curves are due to a Fabry–Perot effect in the thick substrate. One can also observe some strong features in the spectral responsivity. For example on the spectra at ±8°, there is a shoulder at 3.7 μm and a dip at 3.9 μm (black arrows). These features spectrally shift with the angle of incidence. These characteristics have been observed under bias on all the pixels with gratings, but not on pixels without gratings. As a consequence, this effect is not due to an electrical effect, nor to the processing. We attribute it to the optical coupling. We evaluated the peak absorption from joint responsivity and noise measurements. The peak absorption is less than 10%. This value is small in comparison with MW QWIPs on GaAs. So as to understand this small absorption and the spectral features we investigate the optical coupling by means of a modelling approach based on the rigorous coupled wave theory (RCWT) [13–15].

In regular QWIPs the optical coupling is realised through surface waves on a patterned metal surface [16]. In the case of AlInAs/InGaAs on InP, the active layer and the contacts are border by the metal surface on one side, and the InP substrate on the other side, the latter acts as a cladding layer. This waveguide configuration has been studied on GaAs substrates using a thick cladding AlAs layer [17]. It has been demonstrated that the presence of the waveguide strongly affects the coupling. More recently this kind of structures was theoretically investigated [18,19], and it has been shown that there is an important interplay between the surface wave modes in the gratings and the waveguide modes. The result is a dispersion diagram with several modes which are responsible for the observed spectral features in the responsivity.

Using the intersubband absorption as an *in situ* probe of the electromagnetic field polarized along the growth direction, we experimentally investigated the dispersion relations. The frequency was recorded using the FTIR, and the momentum was varied by changing the angle of incidence. So as to get the spectral signature of the coupling, we normalized the responsivity spectra by the responsivity spectrum of a grating-less pixel. The resulting experimental dispersion diagram for a grating period of 1.15 μm is presented in Fig. 2. The dark regions correspond to a low optical coupling efficiency whereas the white regions correspond to a strong coupling.

In an attempt to reduce the angle dependency and optimize the optical coupling, we modelled the dispersion diagram. For the modelling, the pixel is assumed to be infinite along the interfaces. We replaced the two dimensional crossed gratings by one dimensional lamellar gratings. The calculated dispersion diagram is shown in Fig. 3, for a grating period of 1.15 μm.

Besides the approximations, the calculated dispersion diagram agrees remarkably well with the experimental data. All the branches are correctly evaluated. We present in Fig. 4 the electromagnetic field polarized along the growth direction. In the active layer (contacts and absorption layer), the coupling corresponds

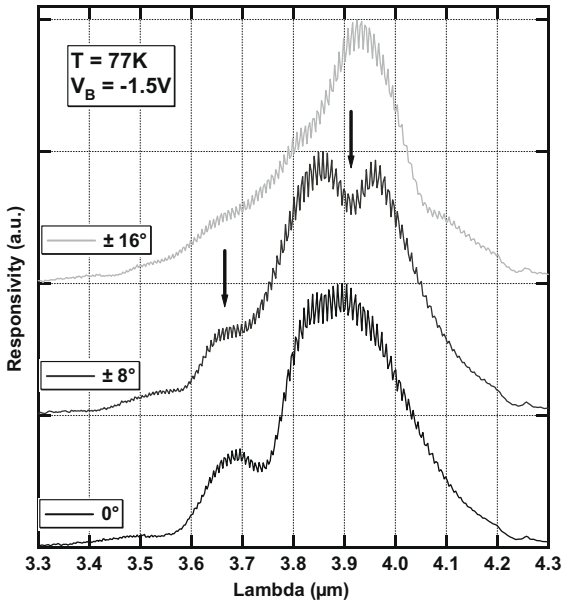

Fig. 1. Spectral responsivity versus the incident angle at 77 K and for an applied voltage (V_B) of -1.5 V. For clarity the spectra are vertically shifted. The arrows highlight some features in the spectra recorded at ±8°.

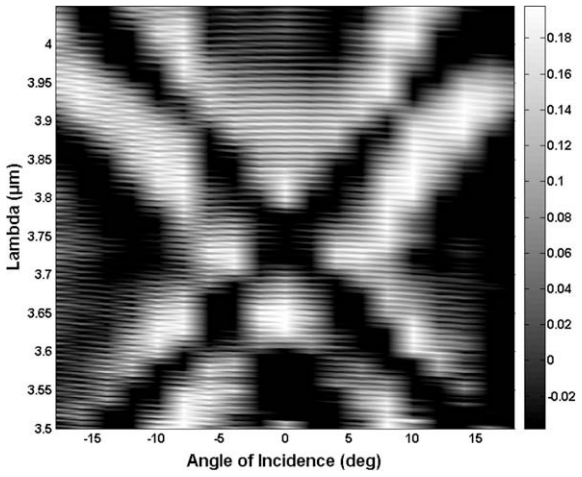

Fig. 2. Experimental dispersion diagram deduced from responsivity measurements on pixel with a grating period of 1.15 μm.